LOW-FIELD NMR PROFILES FOR VERIFICATION OF OIL AND WATER SATURATIONS IN CORES

Christian Straley and Gabriela Leu, Schlumberger-Doll Research Ridgefield, CT 06877

This paper was prepared for presentation at the International Symposium of the Society of Core Analysts held in Trondheim, Norway 12-16 September, 2006

Abstract

This paper has two purposes. Primarily it demonstrates the method and application of low-field NMR for obtaining profiles of saturated or partially saturated rock cores. NMR offers a means of measuring the variation in saturation, which is non-destructive, realistic and easy to implement. Secondarily, this paper examines the potential of centrifuging to prepare partially saturated cores that are uniform in saturation along the length of the core. We are not interested in capillary pressure but want to know how centrifuging restricts saturation-distribution in the preparation of cores for electrical case studies.

Whenever saturation studies are attempted, the method of preparing samples is a concern. We would prefer to use a porous plate method, which leads directly to uniform saturations, but it is often too time consuming. Centrifuging, which is rapid, results in non-uniform saturations as is explained by accepted theory. In this note, our imaging protocol is used to measure NMR profiles for centrifuged samples. The profiles are used to evaluate centrifuging procedures with the goal of attaining uniform saturation.

Conventional NMR is sensitive to hydrogen, which is found in brine or in oil. For oil/brine systems, signals overlap when operating at low field. However, water or oil saturations can be viewed individually by changing the nuclei of one phase. The substitution of D_2O for water makes it possible to observe the hydrocarbon oil saturation directly in oil/brine systems. Alternatively, the use of fluorinated oils and observation of ^{19}F permits the observation of the complementary water and oil saturations with a single sample.

Introduction

Imaging. The phenomenon of NMR (nuclear magnetic resonance) is most widely known through its medical application, MRI (magnetic resonance imaging). Although the imaging capability of NMR is popularly recognized, low-field imaging is used infrequently for laboratory applications to oilfield problems. That could change. There is good reason to expect greater use of NMR imaging in oilfield applications in the future. Because the measurement of diffusion by NMR has become increasingly important, now, many instruments are equipped with single-axis, pulsed, magnetic-gradient sets, which are required for diffusion measurements. The gradient-set also makes it possible to obtain profiles of signal intensity. These simple *images* are effective for quantitative evaluation

of the saturation variation of partially saturated laboratory samples or changes in water content due to porosity variation in the sample.

Recently the NMR experiment, SPRITE, was used [Chen and Balcom, 2005] to evaluate the partial saturation of cores and to measure capillary pressure via a centrifuging experiment. They used a high-field (2.4 *T*) spectrometer. Low-field NMR profiles utilize a simpler experimental alternative and have better sensitivity in most cases [Gravina and Cory, 1994]. SPRITE is preferred when T_2^* is very short, less than one millisecond.

X-ray analysis (DMS) is also used to directly measure saturation of brine and hydrocarbons in cores [Spinler and Maloney, 2001]. These authors note that the limited availability of suitable equipment may prevent widespread application of this technique. Also, to enhance the water signal in order to differentiate it from oil, the water is highly doped. The required doping severely limits the possibility for salinity variation, which is fundamental to electrical studies of partially saturated rock materials and is a major concern for us.

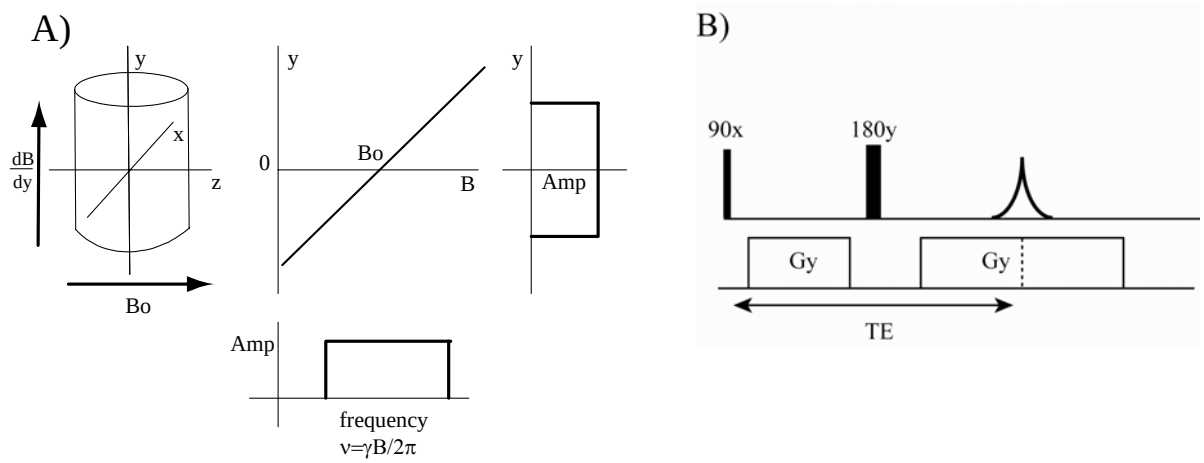

Figure 1: Frame A: For the profiling experiment, the sample is centered in the gradient field. The static field is B_0, which is parallel to the *z*-axis, and the gradient is along the *y*-axis, as shown to the left. When the gradient is turned on, the field in the sample varies along the ordinate. To the right side of the figure is the expected signal amplitude along the y-axis for a homogeneous cylindrical sample. Below, the signal strength is shown as a function of frequency, which is proportional to *B*. Frame B: The data for a profile is produced when a gradient field is applied to encode the position and a second gradient is applied to readout (refocus) the echo.

The profiling experiment is conducted by measuring the signal intensity for a Hahn echo formed after a π/2-τ-π-τ-*echo* sequence while a weak magnetic field gradient is imposed. The change in field is linear along the axis of the sample and the Larmor frequency changes proportionally with the changing field. The PFG (pulsed field gradient) sequence used to collect the Hahn echo with an applied gradient is illustrated in Figure 1. PFG experiments offer advantages over constant gradient experiments.

Turning the gradient off during the π/2 and π pulses, as illustrated, greatly reduces the *r.f.* power requirements. The Fourier transform of the resulting echo results in a broad frequency spectrum in which the local frequency in the sample (often referred to as the phase) varies linearly with the position along the y-axis.

It is advantageous to thoughtfully adjust several parameters used in the profiling experiment involving rock materials when attempting to obtain a quantitative image. Three considerations come to mind immediately. First, because the bound water in rocks can have short relaxation times and because there can be strong internal gradients, it is important to keep the echo time short, which minimizes losses. Second, the sample length must be considered and the applied gradient adjusted accordingly such that the anticipated signal width is matched reasonably to the response function of the probe. If the frequency range of the signal is much larger than the probe's bandwidth, the corrections to the signal at the ends of the sample will be large and will have large, associated uncertainties. Third, the data must be collected with a Nyquist frequency that provides appropriate frequency (spatial) resolution in the profile, according to the precision required of the experiment. The values we settled on are provided in the experimental section.

The NMR magnet and transmitter operate at a specific field and appropriate frequency, although the short hard transmitter pulse will affect hydrogen over a wide range of frequencies. Even with a perfectly uniform magnetic field, placing a core in the field induces internal magnetic gradients arising from susceptibility differences between the rock grains and the pore fluids. These internal gradients lead to an uncertainty regarding the physical origin of the signal for a specific frequency and the frequency information no longer perfectly conveys the spatial information. If the profile is to be useful, it is essential to minimize the uncertainty in the origin of the signal. Because the internal gradients are proportional to the applied field, the uncertainties are smaller for an instrument that uses lower field.

De-saturating by centrifuge. The capillary pressure model for centrifuging is attributed to Hassler and Brunner (1945). Because we are not interested in measuring capillary pressure curves, we are only using HB as a basis for rudimentary discussion. The HB model is uncomplicated. When a cylindrical sample of water-saturated, porous material with a well-connected pore-structure is centrifuged with its axis of symmetry perpendicular to the axis of rotation and with an air/water contact at the base of the sample, the capillary pressure as a function of position is given by:

$$P_c(z) = \frac{\Delta\rho}{2}\omega^2(R_e^2 - (R_e - z)^2). \quad (1)$$

$P_c(z)$ is the capillary pressure at position z above the exit face, Δρ is the wetting phase density minus the non-wetting fluid density, ω is the angular velocity and R_e is the distance from the center of rotation to the exit face of the plug. The maximum capillary pressure is felt at the top of the core, R_t from the axis of rotation, and diminishes, non-

linearly, to zero at the air/water interface at the base of the core, R_e, where 100% saturation should be observed.

Experimentally, many authors have observed that the exit face is not always fully water-saturated. They have pointed to potential causes: a) the use of a water-wet support material [O'Meara et al., 1992]; b) the failure to consider radial pressure profiles found when centrifuging [Fleury and Forbes, 1995]; c) the failure to sleeve the sample [O'Meara et al. 1992]; d) the redistribution of fluids after centrifuging prior to imaging [Baardsen et al., 1991]. Because we are interested in uniform saturation along the length of the core, we welcome all these failure modes into our experiments. When producing water, the samples will be spun unsleeved, on water-wet glass beads, using leisurely profile measurement times.

It is also interesting to consider what would happen if the orientation of the core is reversed. Does the water slosh from one end of the core to the other as if it were in a bucket or does the saturation even out?

Differentiating oil and water in profiles. Saturation profiles from ^1H NMR are not useful when a rock is partially saturated with oil because the signals from the oil and water are indistinguishable. We use two methods to cope with this problem. The first one is to replace the water with D_2O, *heavy water*, which has no signal that can be detected at hydrogen Larmor frequency. The ^1H profile will then reflect only the distribution of oil. A second possibility is to use a fluorinated oil to replace the hydrocarbon oil. Fluorinert oils have a carbon backbone similar to the hydrocarbon oils but all the hydrogen is replaced by fluorine. Fluorine is primarily the ^{19}F isotope, which is a spin 1/2 nucleus. In fact, the ^{19}F resonance is sufficiently close to that of ^1H that our instrument can be tuned to detect fluorine, making it possible to collect the distribution of both phases independently. The ^{19}F signal is weaker than the ^1H signal, about 53% of the water signal per unit volume for the oil that we used, but the profile can be easily calibrated to provide quantitative distributions of the oil phase. Of course, ^1H NMR will provide the distribution of the water phase.

For quantitative work, corrections are necessary to account for T_2 signal losses that occur prior to TE (Echo Time). These losses can be because of short NMR relaxation times of fluids in rock but diffusion in the applied and internal gradient prior to TE might also cause significant losses.

Experimental Methods

NMR. Our NMR experiments were made using two Resonance Instruments spectrometers, a Maran Ultra and a DRX. The instruments operate at a Larmor frequency of approximately 2 *MHz* for hydrogen. The primary instrument had a bore of 40 *mm* while the other had a bore of 50 *mm*. The samples to be tested were 1.5 *in* long and either 1.5 or 0.787 *in* in diameter. The bandwidth of the 40 *mm* probe was approximately 160 *kHz* although the effective bandwidth at the receiver is only 80 *kHz*, which will be

discussed later. A pulsed magnetic field gradient of about 2.5 G/cm was used for profiling. For a sample 1.5 *in* in length, the gradient creates a distribution 40 *kHz* wide. A dwell of 10 μ*s* was used for data collection resulting in a sensitivity to +/-50 *kHz*, more than spanning our anticipated frequency range. Only 256 points were collected, keeping the echo time short. A larger number of points requires a longer echo time since the full evolution of the echo is recorded. As described, the smallest detectable frequency difference is then 390 *Hz* and the profile will span 100 pts rendering a resolution of 0.015 *in*. With these parameters and our spacing, the echo peaks at 6 *ms*. The TE can be reduced further, without loss of signal quality, to 3.5 *ms*, by minimizing the dead time between pulses, if necessary. Still shorter echo time can be achieved if reduced resolution is acceptable; the gradient can be increased and DW can be shortened. Conversely, better resolution is possible if a longer TE is acceptable. When profiling, frequently we used 512 scans, which took 40 minutes and had a typical signal-to-noise ratio, 520:1. A useful profile can be made in 5 minutes with reduced S/N, 180:1.

It is useful to consider the anticipated impact of internal gradients on the profiles. For a Berea sample measured in our instrument, the full signal width is only 200 Hz at half signal power with no applied gradient because the applied field is low. If that signal is described by a normal distribution around a central frequency, 97% of the signal falls within +/- 200 Hz, roughly the size of our profiling bins. In the profile, 97% of the central frequency signal will find its way into the proper bin and the remaining signal will be attributed to adjacent frequency bins, blurring or smoothing the distribution slightly.

For our 40 mm probe, the Fourier transform of the profile echo does not result in a rectangular profile for a cylindrical water sample 1.5 in long. The failure to produce a rectangular profile is because the span of frequencies is roughly equivalent to the effective bandwidth of our probe and filters. A correction is required, which can be created empirically from the water measurement. It is also possible to make a correction using an analytical form for the response function:

$$S = (1+\Delta^2)^{-\frac{1}{2}}, \tag{2}$$

in which $\Delta = \frac{2Q}{f_0} df$, f_0 being the center frequency and *df* the offset in frequency from the center frequency. For our distributions, the analytical expression was used although the value used for the system bandwidth, (f_0/Q), was adjusted empirically to optimize the fit of a water sample profile. Subsequently, that correction was used for all future corrections.

Centrifuging. Centrifuging was done on a Beckmann-Coulter Avanti J-25 centrifuge with a JS-7.5 rotor, which has buckets that swing out horizontally when spinning. The top and bottom of the sample were 6.0 and 9.8 *cm* from the axis of rotation, respectively.

The bottom of the test tube was 15.5 *cm* from the axis of rotation. Several porous supports were tested but most often the base was loose glass beads. We used 50 μm beads initially and larger sizes later; the bead size did not have any obvious impact on the results. The samples were typically spun for 12-24 hours. It took about 5 minutes to get the sample from the centrifuge to the NMR spectrometer.

Results and Discussion

Losses in echo amplitude. There can be three contributions to the loss of signal in profiling experiments. First, there are unavoidable T_1 losses that take place before TE. Second, there are T_2^* losses due to diffusion in the applied gradient before TE. Third, there are losses due to the diffusion in internal gradients before TE. Certainly, the first loss would be anticipated if part of the sample's T_2-distribution is comparable to TE (6 *ms* for these experiments). The magnitude of the first type of loss can be estimated by evaluating the impact of a 6 *ms* delay on the amplitudes of the components of the T_2-distribution for the sample. The second loss, the effect of diffusion in the applied gradient field, can be calculated and is equivalent to only an additional 2.9 second relaxation time and is unlikely to be significant for most samples. The third and last contribution is difficult to estimate although it can be measured because the other contributions are known. A CPMG measured on the decay of the Hahn echo that peaks at TE includes the first and third losses. The comparison of a routine CPMG to the delayed CPMG provides an appropriate correction factor. For Berea, the most significant loss mechanism is found to be diffusion in the internal gradients. This reinforces the fact that it is important to use as short a TE as possible.

Porosity from profiles. Figure 2 shows the profile for a Berea 500. The corrected profile is roughly rectangular in shape as expected for a homogeneous material. The ordinate is proportional to the water content or saturation and the frequency (abscissa) is linearly related to the position. Because the rock is fully saturated, the total area is proportional to the porosity.

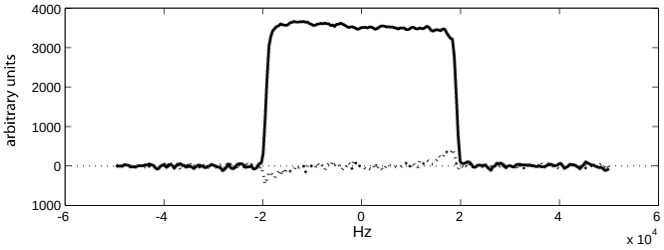

Figure 2: This profile is the Fourier transform of the quadrature echo data for Berea 500. The use of phased data has some limitation. The dotted black line indicates the out-of-phase signal and the excessive noise (horns) under the sample area reflect the inability to resolve the phase rotation exactly. A difference in frequency of 1Hz represents 9.4×10^{-5}cm.

^{1}H NMR mass measurements require a secondary calibration. In other words, NMR mass measurements are calibrated to a standard sample measured using the experiment of interest and parameter settings that are to be used for the sample itself. The mass of hydrogen in the sample is found by comparison of the corrected signal strength of the sample to the corrected strength of the standard and multiplying by the mass of hydrogen in the standard. The errors discussed in the previous example affect both the standard and the sample and must be properly taken into account to find the correct mass of hydrogen and to evaluate the uncertainty in the profile. If the fluid changes, the hydrogen index must be considered, too.

To correct profiles and to achieve quantitative saturation, it is necessary to record a normal CPMG and a delayed CPMG starting from the echo time for the standard and for the sample, as well. The buoyancy porosity is in good agreement with the NMR porosity by CPMG. We found the CPMG of a Hahn echo to have a loss of 6.4, 11 and 12% for the standard and two of our study samples, respectively, due to the causes discussed above. The standard requires a 6.4% correction and the samples 11 and 12% corrections before calculating the mass of water. The total porosity determination from the profile agrees well with the buoyancy porosity after the correction for the Hahn echoes' signal-loss; the agreement was to within 0.3 porosity units for the total porosity.

This Berea sample is uniform and the ordinate of the profile can be converted to porosity using the volume of the sample and the required corrections. Of course, a porosity value for each slice in the profile exists, which in the case of Berea is roughly constant. A non-uniform sample, with laminations perpendicular to the y-axis, might present problems in establishing the accurate porosity or saturation. We used a single correction factor in these cases although it is possible to conceive other schemes.

Profile Resolution. As was explained earlier, the standard resolution in these experiments has been 0.015 *in* but higher resolutions are possible. To achieve higher resolution, a longer echo time is required. Figure 3 provides a comparison of a layered sample measured at our standard resolution and at a resolution a factor of four higher. The profiles can be compared to visual clues from the included core photo. The dark stripe at left correlates well with a region of depressed porosity. Stripe to the right side are less easily correlated but there are clear possibilities. The sand on the right hand side of the plug has a different color and the porosity on that side is depressed. In general, the features in the profile reflect the features in the photo.

Comparing the profiles in Figure 3, the boundaries are sharper and details are revealed in the higher resolution profile while the coarse delineation of features are similar. The amplitude of the better-resolved profile is diminished, however. The loss of amplitude is expected because of the longer echo time required for the higher resolution profile (21 *ms*). Comparison of the amplitudes of the Hahn echoes show that 90% of the full signal is seen in the lower resolution profile and only 70% of the potential signal is seen in the

higher resolution profile. Larger uncertainties should be anticipated in the porosity distribution for the higher resolution measurement because of the larger correction required.

Air/water saturation. Samples partially saturated with water/air are easy to evaluate; NMR sees only the water and the profile will reflect the distribution of the water. Of course, amplitude corrections of the type discussed earlier are necessary to obtain quantitative saturation. HB's or Korringa's theories assign the proper capillary pressure, not saturation, as a function of position. Fortunately, mercury porosimetry can be used to relate the capillary pressure to the saturation and allows us to evaluate our measured saturation in comparison to the model saturation. Figure 4 includes theoretical saturation curves to evaluate the correspondence to theory.

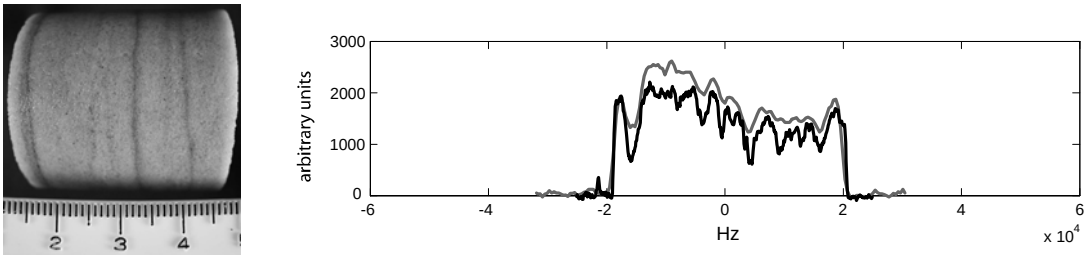

Figure 3: The left frame is a photograph of a sandstone with laminations roughly perpendicular to the central axis of the plug. The dark colored striation at left correlates nicely with the NMR saturation profiles in the right frame. In that frame the spectral (linear) resolution of the black curve is four times finer than that of the grey curve.

Effects of centrifuging. Provided centrifuging speeds are low, regions of 100% water saturation are maintained above the exit face and the profile behaves roughly as required by the HB model. Of course, our goal has been different, historically. We have not used centrifugation to measure capillary pressure but used it to reduce the saturation to irreducible levels. Years ago, in our lab, a crude evaluation comparing the magnitude of frequency selected slices in a core indicated that S_{Wirr} achieved by centrifuging was relatively uniform. Our samples were placed directly on glass beads with the hope of displacing the air/water contact and left unsleeved. Now, with this simple profiling, we can confirm that at high centrifuging speeds, the irreducible saturation is found to be relatively uniform.

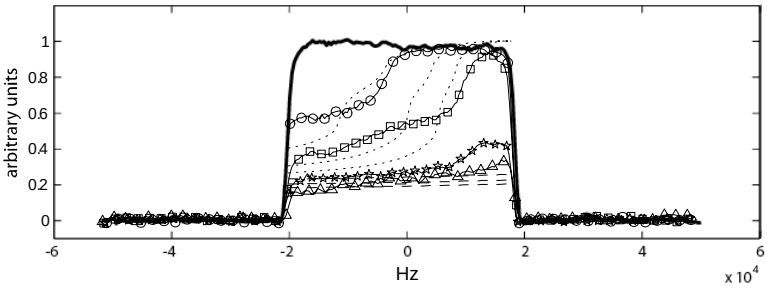

Figure 4: The black curve is the profile for Berea 500 when fully saturated. The curve with circles was desaturated at HB 2.21 *psi* (680 *rpm*) for 20 hours. 3.37 *psi* (840 *rpm*) is the curve marked by squares. Stars indicate 4.77 *psi* (1000 *rpm*) and triangles show the effect of reversing the plug's orientation in the centrifuge (at 4.77 *psi*). The dotted curves show the anticipated saturation profiles from mercury porosimetry and using HB at the three pressures while the dashed curves indicate the result anticipated by Korringa.

In our study we do not try to maintain conditions that would create theoretical HB curves. Figure 4 indicates the degree to which HB seems to be relevant for our conditions. The results of several centrifuge experiments and the anticipated saturation curve calculated from Equation 1 and mercury porosimetry are shown. The saturation curves anticipated by Korringa are also included (Wunderlich, 1985). These curves assume thermodynamic equilibrium and that $P_c=0$ at the air/water interface, far below the exit face of the core. At the lowest spinning speed, 2.21 *psi*, which left a water saturation of greater than 80%, there is rough agreement with HB. At 3.37 *psi* the water saturation is significantly less than expected and at 4.77 *psi* the end of the plug is significantly desaturated and the profile seems to be in better agreement with the Korringa style estimate. The saturation is rather uniform and is less than 25%. Redistribution of fluids may contribute to the uniformity in that it took up to 45 minutes to complete the measurement after spinning. However, Baardsen et al, (1991) indicated that redistribution was a slow process, requiring days, which was our experience as well.

It is interesting to ask whether uniform saturation could be achieved at high values of saturation by reversing the orientation of the core. The experiments in Figure 5 try to answer this question. Upon reversal at low capillary pressures, only the ends are partially desaturated. The initial desaturation is not reversible and remains despite the inversion of the core. The overall saturation is not uniform in the least. At higher capillary pressure the desaturated regions merge and can provide somewhat uniform saturation across the plug. For this sample, the merge occurs at about 50% saturation although there is a dimple in the middle of the saturation profile, which is an artifact of the conditions. This experiment suggests that higher saturations will be even more non-uniform. Desaturation by centrifuging to produce uniformly saturated samples is viable at lower water-saturations but does not seem useful for higher water-saturations.

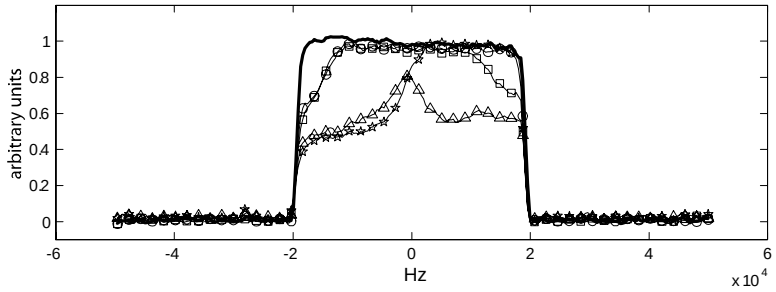

Figure 5: This Berea 500 plug was unsleeved and spun on unconsolidated glass beads. The continuous black curve is the profile for the fully saturated core. The line with circles indicates the saturation at 1.00 *psi* and the squares show the effect of reversing the orientation of the core and re-centrifuging. The stars show the saturation at 1.72 *psi* and the triangles show the effect of reversing the orientation (at 1.72 *psi*).

Oil/D_2O saturations. Using D_2O to replace water in a partially hydrocarbon oil-saturated sample permits the unambiguous evaluation of the oil saturation and distribution. An example of this is given in Figure 6. In this case the rock was initially saturated with D_2O and dodecane was used to displace the D_2O using the centrifuge. It is also possible to replace water with D_2O through diffusive dilution [Morriss et al., 1994].

In Figure 6 the oil peak in the rock is shifted to faster relaxation times relative to the bulk oil peak. This indicates that the oil is contacting the surface of the rock and is wetting the rock. This indicates that the rock is partially oil wet. A difference will be seen between this case and the one that will be shown in the next section, where fluorinert oil shows no shift and may indicate a non-wetting invasion.

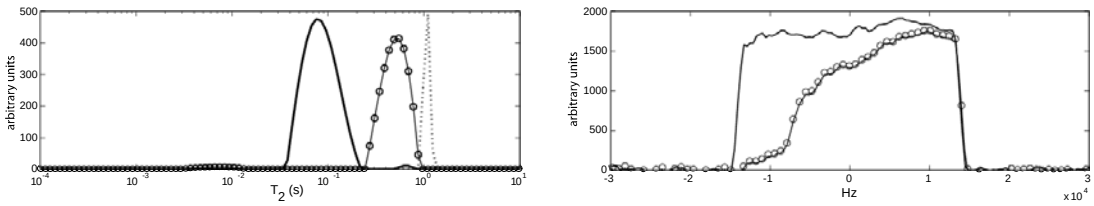

Figure 6: The left frame shows CPMG data and the right frame shows saturation profiles of dodecane for a sandstone rock. The continuous black curves are for the fully brine saturated sandstone. After centrifuging at 81 *psi*, the curve with circles indicates the dodecane. In the left frame the doted black curve is for bulk dodecane.

Fluorinert-oil/water saturations. The gyromagnetic ratio for ^{1}H is 26,752 s^{-1} while for ^{19}F it is only 25,167 s^{-1}, which means that at the same field the resonance of ^{19}F is at 94.075% of the frequency of ^{1}H. Our ^{1}H spectrometers allow us to operate at the frequency of ^{19}F; the transmitter has sufficient range and the probe's capacitor has enough range to adjust its tuned circuit. ^{19}F is 100% abundant, second only to hydrogen in its NMR sensitivity, which is 83% that of hydrogen for the same spin density. Of course, with the frequency selectivity of our instrument, the ^{19}F and the ^{1}H measurements are completely independent and non-interfering. The signal strength for either nuclei is given by

$$S \propto \frac{\gamma^4 B_0^2 N B_{1\perp} \hbar^2}{kT}. \qquad (3)$$

Fortunately, $B_{1\perp}$ can be related to the measured $\pi/2$ pulses found through $\pi/2 \propto \gamma B_{1\perp} t_{90}$ and from the previous equation it is possible to anticipate the signal strength of ^{19}F relative to ^{1}H, which would be the ratio of the equation for fluorine divided by the equation for hydrogen. Of course, many of the terms cancel, leaving

$$\frac{S_F}{S_H} = \frac{\gamma_F^3}{\gamma_H^3} \times \frac{t_{90H}}{t_{90F}} \times \frac{N_F}{N_H}. \qquad (4)$$

The sensitivity term mentioned previously comes from the comparison of the gyromagnetic ratio raised to the power of three. From our experiments, t_{90H}=16.1 μs and t_{90F}=*17.8* μs. All that is left is to evaluate the spin concentration terms.

The relative density of spins can be found empirically or can also be calculated when the density and molecular formula are known. FC-77 was selected for our oil because it has a viscosity of 1.42 *cP* at 25^{o}C. The boiling point, 97 ^{o}C, is high enough that evaporation

should not be a problem. For FC-77, the density is 1.78 *g/cm*^{3} and the average molecular weight is 415. If we assume that it is a normal saturated compound (no branching) the formula for a basic two-fluorine unit is $C_{0.88}F_{2.00}$ with a formula weight of 48.61. Using the density, we find that there are 0.66 formula units for each molecule of water, the third ratio required for the estimation of the relative strength of the ^{19}F signal. Overall, using FC-77, our fluorine signal should be 52.8% of the strength of the ^1H signal of a water sample of equal volume. The relative strength of the signal is confirmed by CPMG experiments on hydrogen and fluorine standards that show a relative strength of 53.4%.

Figure 7 illustrates the complimentary nature of the ^1H and ^{19}F NMR measurements. Although the oil saturation could be assumed to be the missing saturation from the ^1H measurement, it is reassuring to actually see the oil profile and agreement with the fully saturated sample. This sample was a 2 *cm* diameter core, 3.75 *cm* in length. The profiles appear to be shorter compared to the other measurements included. These distributions were run inadvertently using a gradient strength of 1.75 *G/cm* rather than the 2.5 *G/cm* used for other tests. In this case, to a frequency difference of 1Hz corresponds 1.34×10^{-4}cm. For some of the profiles, the edges do not align well. This problem could probably be cured by improving the core holder such that the sample would be returned to its correct position more precisely.

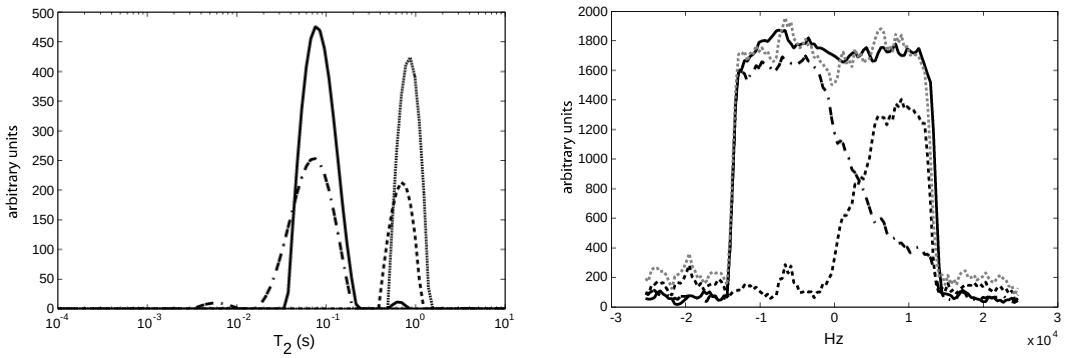

Figure 7: The left frame shows CPMG data and the right frame shows saturation profiles for a sandstone rock. The continuous black curves are for the fully brine saturated sandstone. After centrifuging at 81 *psi* in fluorinert, the black dotted line (large dots) indicates the fluorine curve and the dotted-dash line indicates the hydrogen curve. In the left frame the large grey peak is for bulk FC-77 and in the right frame, the grey dotted curve is the sum of the hydrogen and fluorine profiles. The amplitude of the grey dotted curve has been boosted as described in the text to have a porosity scale comparable to water.

Conclusions

Low-field NMR profiling can be widely useful in core analysis to provide oil or water saturation and distribution. Increasingly available, low-field NMR-instruments, equipped with a PFG unit, are capable of creating profiles easily. Our instrument, which operates at 2 MHz can measure profiles from ^1H or ^{19}F. The profiles are quantitative when the data is collected properly.

Saturations established through centrifuging are generally non-uniform as anticipated by HB or Korringa's theory. The actual distribution expected by HB is not always found. If the cores are unjacketed and rest on water-wet glass beads, the air/water contact with $P_c=0$ can be displace from the exit face of the core although Korringa's thermodynamic equilibrium does not appear to be reached. In general, relatively uniform saturations can be achieved at irreducible or low water-saturation while it does not seem possible to achieve high, uniform saturation.

The use of D_2O rather than water allows the measurement of oil distribution unambiguously; in ^1H NMR, deuterium is invisible. The replacement of the hydrocarbon-based oil with fluorinert allows the measurement of complementary oil and water saturations. ^{19}F NMR with fluorinert is not, however, an exact analogy to hydrocarbon oil. Fluorinert, which is neither oil nor water soluble, has different wetting characteristics than either oil or water. This is illustrated by the difference between oil/water and fluorinert/water T_2-distributions found in this paper for a partially oil-wet carbonate.

References

Chen, Q., Balcom, B.J., "Measurement of rock-core capillary pressure curves using a single-speed centrifuge and one-dimensional magnetic-resonance imaging", *J. Chem. Phy*., (2005) **122**(21), Art. No. 214720.

Fleury, M. and Forbes, P., "Radial effect and sample heterogeneity effect on centrifuge capillary pressure curves", In *Trans SCA Con*., (1995), Paper 9534.

Gravina, S., Cory, D.G., "Sensitivity and resolution of constant-time imaging", *J. Magn. Res., Series B*, (1994), **104**, 53-61.

Hassler, G. L., Brunner, E., "Measurement of Capillary Pressure in Small Core Samples", *Trans. Am. Inst. Min. Metall. Eng.*, (1945), **160**, 114–123.

Morriss, C.E., Freedman, R., Straley, C., Johnson, M. Vinegar, H.J., Tutunjian, P.N.,"Hydrocarbon saturation and viscosity estimation from NMR logging in the Belridge Diatomite", In *Trans. SPWLA Annu. Log. Symp*., (1994), Paper C.

O'Meara Jr., D.J., Hirasaki, G.J., Rohan, J.A, "Centrifuge measurements of capillary pressure: Part - outflow boundary condition", *SPE Reservoir Engineering*, (1992).

Wunderlich, R.W., "Imaging of wetting and non-wetting phase distributions: Application to centrifuge capillary pressure measurements", In *60th Annual Technical Conference and Exhibition*, (1985).